UC Davis
UC Davis Previously Published Works

Title

Molecular Characterization of Organosulfates in Organic Aerosols from Shanghai and Los Angeles Urban Areas by Nanospray-Desorption Electrospray Ionization High-Resolution Mass Spectrometry

Permalink

https://escholarship.org/uc/item/3hs205t6

Journal

Environmental Science and Technology, 48(18)

ISSN

Authors

Tao, Shikang
Lu, Xiaohui
Levac, Nicole
et al.

Publication Date

2014-09-16

DOI

Peer reviewed

High-Resolution Mass Spectrometry and Molecular Characterization of Aqueous Photochemistry Products of Common Types of Secondary Organic Aerosols

Dian E. Romonosky,[†] Alexander Laskin,[‡] Julia Laskin,[§] and Sergey A. Nizkorodov*,[†]

[†]Department of Chemistry, University of California, Irvine, California 92697, United States

[‡]Environmental Molecular Sciences Laboratory and [§]Physical Sciences Division, Pacific Northwest National Laboratory, Richland, Washington 99352, United States

S *Supporting Information*

ABSTRACT: This work presents a systematic investigation of the molecular level composition and the extent of aqueous photochemical processing in different types of secondary organic aerosol (SOA) from biogenic and anthropogenic precursors including α-pinene, β-pinene, β-myrcene, D-limonene, α-humulene, 1,3,5-trimethylbenzene, and guaiacol, oxidized by ozone (to simulate a remote atmosphere) or by OH in the presence of NO_x (to simulate an urban atmosphere). Chamber- and flow-tube-generated SOA samples were collected, extracted in a methanol/water solution, and photolyzed for 1 h under identical irradiation conditions. In these experiments, the irradiation was equivalent to about 3−8 h of exposure to the sun in its zenith. The molecular level composition of the dissolved SOA was probed before and after photolysis with direct-infusion electrospray ionization high-resolution mass spectrometry (ESI-HR-MS). The mass spectra of unphotolyzed SOA generated by ozone oxidation of monoterpenes showed qualitatively similar features and contained largely overlapping subsets of identified compounds. The mass spectra of OH/NO_x-generated SOA had more unique visual appearance and indicated a lower extent of product overlap. Furthermore, the fraction of nitrogen-containing species (organonitrates and nitroaromatics) was highly sensitive to the SOA precursor. These observations suggest that attribution of high-resolution mass spectra in field SOA samples to specific SOA precursors should be more straightforward under OH/NO_x oxidation conditions compared to the ozone-driven oxidation. Comparison of the SOA constituents before and after photolysis showed the tendency to reduce the average number of atoms in the SOA compounds without a significant effect on the overall O/C and H/C ratios. SOA prepared by OH/NO_x photooxidation of 1,3,5-trimethylbenzene and guaiacol were more resilient to photolysis despite being the most light-absorbing. The composition of SOA prepared by ozonolysis of monoterpenes changed more significantly as a result of the photolysis. The results indicate that aqueous photolysis of dissolved SOA compounds in cloud/fog water can occur in various types of SOA, and on atmospherically relevant time scales. However, the extent of the photolysis-driven change in molecular composition depends on the specific type of SOA.
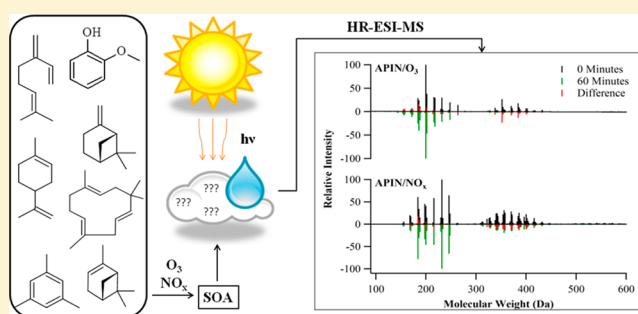
I. INTRODUCTION

Primary and secondary organic aerosols (POA and SOA) influence the Earth's climate and contribute to air pollution in urban areas.[1,2] POA are directly emitted, whereas the more abundant SOA are produced in one of the following ways: (1) gas-phase oxidation of volatile organic compounds (VOCs) followed by condensation of the products into new particles or onto preexisting particles;[3,4] (2) heterogeneous reactive uptake of VOCs on particle surfaces;[5] (3) photochemical aqueous processing of VOCs occurring inside cloud and fog droplets, followed by droplet evaporation.[6,7] Until recently, the first pathway was thought to be the main mechanism of SOA formation and attracted significant attention from the scientific community. Numerous studies have contributed to a comprehensive compilation of reference tables of photo-chemical and kinetic data for hundreds of VOCs[8] and in tabulation of SOA yields[9] from oxidation of different VOC precursors by the hydroxyl radical (OH), ozone (O_3), and the nitrate radical (NO_3). In the past several years, it has been recognized that a significant fraction of SOA is produced and subsequently aged through cloud and fog photochemical processes.[7] This represents a significant shift in scientific knowledge of the SOA chemistry, and new data are required to assess the relative contribution of aqueous processes to SOA formation and aging.
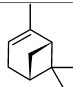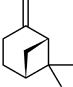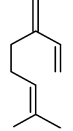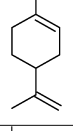
Photochemical processes involving organic compounds in cloud and fog water include direct photolysis, wherein the compounds absorb radiation and break into products, and indirect photooxidation, wherein absorption of solar radiation drives chemistry through the production of oxidants such as OH, superoxide (O_2^-), and electronically excited organic compounds. Direct photolysis processes are well-known to determine lifetimes of many gas-phase species,[2] and they are likely to be just as important for compounds found in the pa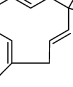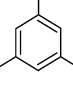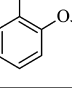rticle phase and in cloud/fog droplets. Oxidation by OH is the primary competitive channel for photolysis. However, in cloud and fog water affected by urban emissions, as well as inside organic aerosol particles, the oxidative capacity of OH may be too low to oxidize the high concentrations of all dissolved SOA during the cloud/fog lifetime.[7] Additionally, the higher dissolved SOA concentrations may suppress photochemical OH production enough to shut down the OH-initiated loss pathway chemistry while not affecting the direct photochemical pathways. Dissolved organics may also serve as a source of OH through the photolysis of nitrates, H_2O_2, and organic chromophores.[7,10,11] Depending on the prevailing mechanisms, aqueous photochemistry can both degrade dissolved organic compounds into smaller volatile products or conversely generate larger, nonvolatile products. For example, previous studies demonstrated that OH-driven oxidation of small water-soluble organics often leads to a complex and concentration-dependent mixture of oligomeric compounds.[12−16] Formation of oligomeric products was also observed in the photolysis of aqueous pyruvic acid.[17,18] In contrast, the photolysis of aqueous solutions of model SOA prepared by the oxidation of isoprene, limonene, and naphthalene was found to lead to photodegradation of larger organics into smaller products.[15,19,20]

Direct and indirect photolysis processes occur simultaneously, but their relative importance can be predicted only for the simplest organic compounds, which are not representative of SOA composition.[21] While much attention has been given to the aqueous oxidation of organic compounds with the OH radical,[7] there is limited knowledge about the direct photolysis of atmospherically relevant organics in water, especially for processes involving multifunctional organic compounds. Furthermore, it is important to study the response of complex aqueous mixtures to irradiation (as opposed to solutions of isolated compounds which may behave differently from the mixtures) since they are more representative of cloud and fog chemistry. Finally, little is known about the photochemistry of SOA-relevant multifunctional organic compounds such as highly substituted carbonyls, organonitrates (esters of nitric acid), and organosulfates (esters of sulfuric acid), etc., which are common in SOA but challenging to synthesize and study in pure form.

In this work, we investigate the effects of aqueous photolysis on the molecular level composition of different representative types of SOA of both biogenic and anthropogenic origin (Table 1). We use high-resolution mass spectrometry (HR-MS) methods[22] to analyze changes in SOA composition upon exposure to UV radiation. In addition, we compare high-resolution mass spectra of various types of SOA, something that has not been done systematically in previous literature. Biogenic SOA precursors include α-pinene, β-pinene, myrcene, and D-limonene, which are among the top six most abundant monoterpenes in the atmosphere.[23] A product of diesel combustion, 1,3,5-trimethylbenzene,[24] and a product of

Table 1. Structures of VOC Precursors Used for the Generation of SOA Samples, Abbreviations by Which They Are Referred to in This Work, and Their Commercial Sources and Purities

Compound	Abbreviation	Manufacturer/Purity	Structure
α-Pinene	APIN	Sigma Aldrich, 98%	
β-Pinene	BPIN	Sigma Aldrich, 98%	
β-Myrcene	MYR	Fisher Scientific, 92.9%	
(+)-Limonene	LIM	Sigma Aldrich, 97%	
α-Humulene	HUM	Sigma Aldrich, >96%	
1,3,5-trimethylbenzene	TMB	Sigma Aldrich, 5000 μg/mL in methanol	
Guaiacol	GUA	Sigma Aldrich, >98%	OH

biomass burning, guaiacol,[25] are included as model anthropogenic and biomass-burning precursors. The oxidants include ozone, which controls the oxidation of many unsaturated organics in clean air, and OH in the presence of NO_x (=NO + NO_2) concentration, which is representative of an urban environment. In combination with previous studies of aqueous photolysis of limonene, isoprene, and naphthalene SOA,[15,19,20] this study provides a database for making general conclusions about the role of aqueous photochemistry in the atmospheric processing of SOA.

II. EXPERIMENTAL SECTION

Both O_3-initiated and OH/NO_x-initiated oxidation experiments were performed to generate SOA from suitable biogenic and anthropogenic VOCs. All of the OH/NO_x photooxidation SOA are labeled as VOC/NO_x and ozonolysis SOA are labeled as VOC/O_3 in the remainder of this work. Conditions for each experiment and code names for the SOA are summarized in Table 2. For the OH/NO_x-initiated reactions, the photooxidation of VOC precursors was performed in a ∼5 m³ Teflon chamber under dry conditions in the absence of seed particles with approximately 300−400 ppb NO added to the chamber. Hydrogen peroxide (H_2O_2) was used as the OH precursor. A measured volume of H_2O_2 (Aldrich; 30% by volume in water) was added by evaporation with a stream of zero air to achieve 2 ppm of H_2O_2 in the chamber. VOC precursors were added in the same manner, and the chamber content was mixed for several minutes using a fan, which was shut off after mixing to

Table 2. Experimental Conditions and Code Names for the SOA Samples Examined in This Work

SOA code[a]	oxidant	initial VOC (ppm)	initial NO (ppb)	reacn time (h)	collecn time (h)	amt collected (μg)
APIN/O$_3$	O$_3$	~5	0	<0.1	1	930
APIN/NO$_x$	OH	0.80	330	2	3	460
BPIN/O$_3$	O$_3$	~5	0	<0.1	1	260
BPIN/NO$_x$	OH	0.80	360	2	3	1900
LIM/O$_3$	O$_3$	~5	0	<0.1	1	1300
MYR/O$_3$	O$_3$	~5	0	<0.1	1	170
MYR/NO$_x$	OH	0.50	370	3	3.5	1200
HUM/O$_3$	O$_3$	~5	0	<0.1	1	470
HUM/NO$_x$	OH	0.25	260	3	2.5	90
GUA/NO$_x$	OH	0.50	360	1	3	2600
TMB/NO$_x$	OH	0.090	440	6	4	30

[a]The OH/NO$_x$ photooxidation SOA are labeled as VOC/NO$_x$ and ozonolysis SOA are labeled as VOC/O$_3$. All of the VOC/NO$_x$ samples were prepared in a smog chamber starting from the specified initial mixing ratios, and all of the VOC/O$_3$ samples were prepared in a flow tube. Steady state mixing ratios that the VOC precursor would have had in the absence of ozone are listed (ozone was added to the flow in excess with respect to the VOC). The reaction time in the flow tube is estimated from the effective residence time; the reaction time in the chamber is equivalent to the irradiation duration.

minimize wall losses. UV-B lamps (FS40T12/UVB, Solarc Systems Inc.) with emission centered at 310 nm, were turned on to initiate the photochemistry. SOA particles formed in the chamber were monitored by a TSI model 3936 scanning mobility particle sizer (SMPS), while a Thermo Scientific model 49i ozone analyzer and a Thermo Scientific model 42i-Y NO$_y$ analyzer recorded O$_3$ and NO/NO$_y$ data, respectively. The SOA was collected through an activated carbon denuder at 30 SLM (standard liters per minute) onto poly-(tetrafluoroethylene) (PTFE) filters (Millipore 0.2 μm pore size). Two hours of collection yielded 30−1900 μg of SOA on each filter (the amount was estimated from the SMPS data assuming a generic SOA particle density of 1.2 g cm^{-3} and 100% collection efficiency by the filters) before it was sealed and frozen for further analysis.

The O$_3$-initiated reactions were carried out in a 20 L flow tube reactor under dry conditions at atmospheric pressure and room temperature.[26] The liquid VOC precursor was injected in a 5−7 SLM flow of zero air at a rate of 25 μL/h using a syringe pump. Pure oxygen (Airgas; 99.994% purity) flow of ~0.6 SLM passed through an ozone generator and a photometric ozone detector. The two flows were mixed at the entrance of the flow tube resulting in the initial VOC and ozone mixing ratios of ~5 ppm and 50−100 ppm, respectively. The residence time in the flow tube was less than 5 min but sufficient for oxidizing all of the injected VOC and forming SOA. A 1 m long charcoal denuder removed residual ozone and gaseous organic compounds from the flow exiting the reactor while letting most of the particles go through. The SOA was collected for approximately 2 h on PTFE filters which were weighed before and after collection with a Sartorius ME-5F filter balance (1 μg precision), then sealed, and frozen for later analysis.

The sealed filter samples were allowed to equilibrate to room temperature, unsealed, and extracted by a 70/30 methanol/water v/v solution for about 10 min using sonication. The methanol/water extracts prepared in this manner had typical concentrations of organics in the range of 50−250 μg/mL, which corresponds to 170 μM − 800 μM, assuming an effective molecular weight of 300 g/mol for SOA compounds. The concentrations used in this study are comparable to concentrations of organic compounds observed in cloud-water.[27,28] Deliquesced atmospheric particles typically have higher concentrations of dissolved organics of the order of 0.1− 10 M.[29] Therefore, the experimental conditions presented in this study are more relevant for cloud and fog droplets than for hygroscopically grown aerosols.

Methanol was added to ensure a more complete extraction of the SOA material from the filters, and to improve the stability of the electrospray ionization (ESI) source used in the composition analysis before and after photolysis. Our initial intention was to study photolysis in pure water, but this was not possible for example for HUM/O$_3$, which (similarly to cedrene)[30] dissolved poorly in water but dissolved readily in methanol. Although methanol is known to react with SOA carbonyl compounds to form hemiacetals,[31] this reaction is expected to have a similar effect on the photochemical
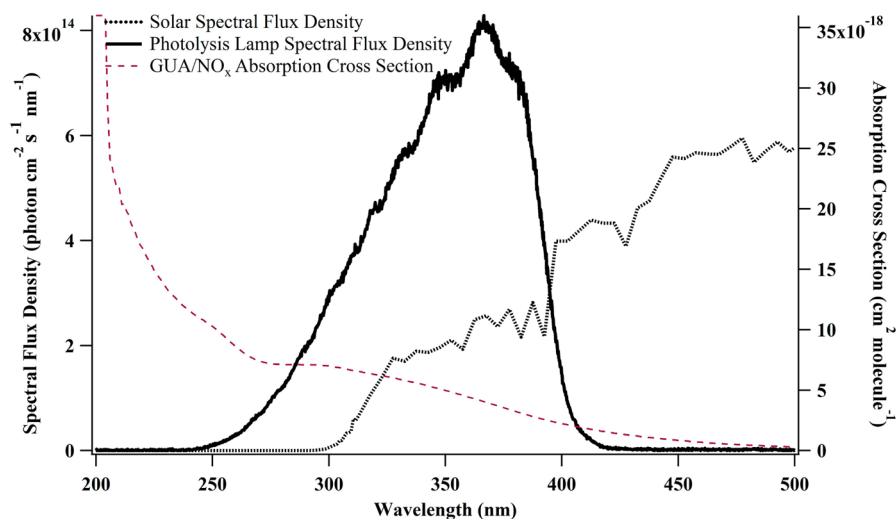

Figure 1. Spectral flux density in the photolysis cuvette compared to the solar spectral flux density at SZA = 0. The right axis shows the effective absorption cross-sections of GUA/NO$_x$ calculated from eq 1.

properties of carbonyls (an elimination of the n → π* transition associated with the carbonyl group) as the hydration reaction with water leading to gem-diols. Therefore, in first-order approximation, photochemistry of SOA in water and in methanol/water mixtures should be qualitatively similar.

The samples were photolyzed in a 1 cm uncapped quartz cuvette from the side. A Xenon UV lamp in a Newport model 66902 housing served as the radiation source. A 90-degree dichroic mirror (Newport model 60159) and a U-330 band-pass filter (Edmund optics #46−438) were used to reduce the visible and IR radiation. The spectrum of the resulting radiation was recorded using a portable UV−vis spectrometer (Ocean Optics, USB4000) with most of the radiation falling in the 280−400 nm range. The samples were exposed to lab air during photolysis and therefore contained dissolved oxygen. After photolysis, the samples were placed into clean storage vials and frozen for later mass spectrometric analysis. An azoxybenzene actinometer was used under the same experimental conditions to determine the flux of the lamp as described by Lignell et al.[32]

The wavelength-dependent spectral flux density in the photolysis cuvette is shown in Figure 1, where it is compared to the ground-level spectral flux density from the sun at solar zenith angle (SZA) of 0° (calculated with the "Quick TUV" calculator[33] using the following parameters: 300 Dobson overhead ozone, surface albedo of 0.1, ground elevation and altitude =0 km). We also show the effective absorption cross sections of GUA/NOx SOA determined in this work from the following equation,

$$\sigma_{\text{effective}}(\lambda) = \frac{A_{10}(\lambda)\ln(10)\text{MW}}{C_{\text{mass}}N_{A}l} \tag{1}$$

where N_A is Avogadro's number, A_{10} is base-10 absorbance of an SOA extract with mass concentration C_{mass} contained in a cuvette with path length l. We used MW = 300 g/mol for the effective molecular weight of GUA/NO$_x$ SOA molecules (the average molecular weight of all the compounds detected by HR-MS in all the SOA types). GUA/NO$_x$ SOA was the most absorbing compared to the rest of SOA probed here (its samples were yellow in color; the rest of the SOA samples were colorless). The ratio of the relative rates of photolysis by the lamp under our experimental conditions and by the sun can be estimated from

$$\frac{J_{\text{sun}}}{J_{\text{lamp}}} = \frac{\int \sigma_{\text{effective}}(\lambda)\,\phi(\lambda)\,\text{flux}_{\text{sun}}(\lambda)\,\text{d}\lambda}{\int \sigma_{\text{effective}}(\lambda)\,\phi(\lambda)\,\text{flux}_{\text{lamp}}(\lambda)\,\text{d}\lambda} \tag{2}$$

assuming that only wavelengths below 400 nm contribute to photolysis, and assuming that the photolysis quantum yield ϕ is wavelength-independent. The assumption of the constant ϕ is certainly an approximation, but this is a practical approach based on the limited available information on photophysics of SOA compounds. With these assumptions, we estimate that 1 h of photolysis by the lamp is equivalent to ~4 h of photolysis with the overhead sun. Note that this ratio depends on the shape (but not the magnitude) of the absorption cross sections of SOA. For example, for APIN/O$_3$ SOA, which is much less absorbing at λ > 300 nm, the 1 h of lamp irradiation would be equivalent to ~8 h of irradiation by the sun in its zenith. Note that our lamp has a measurable emission at λ < 290 nm according to Figure 1. With the integration wavelength limited to λ > 290 nm, the effective solar exposure time for GUA/NO$_x$ SOA becomes ~3.5 h, while that for APIN/O$_3$ SOA becomes

~5.5 h. Therefore, the measured photolysis rates may be affected by the contribution of harder UV (λ<290 nm) to some extent. A more thorough analysis of photolysis rates by different SOA types under different environmental conditions will be presented elsewhere.

Extracted SOA samples were analyzed before and after photolysis using a high-resolution LTQ-Orbitrap mass spectrometer equipped with a modified ESI source.[15,19,34−38] Mass spectra of the solvent were also collected in order to subtract from the sample mass spectra during the data analysis stage. Mass spectra were acquired in the positive ion mode for all samples. The instrument was operated at the resolving power of 10^5 $m/\Delta m$ at m/z 400.

To process the large number of mass spectra recorded during this work, data analysis was performed similarly to our previous work.[36−38] For each spectrum, a list of peak positions and intensities was generated using Decon2LS (http://omics.pnl.gov/software/decontools-decon2ls). The resulting peak lists for all the files in the same experimental batch, including blank samples, were first assigned with a m/z tolerance of ±0.001 to molecular formulas C$_c$H$_h$O$_o$N$_n$Na$_x^+$ (small letters c, h, o, n refer to the number of corresponding atoms in the ion; the number of Na atoms x is restricted to 0 or 1). Constraints were imposed on the elemental ratios (0.05 ≤ o/c ≤ 1.3, 0.7 ≤ h/c ≤ 2.0) and parities (c-(h+x)/2+n/2 + 1 must be half-integer for closed-shell protonated or sodiated molecules). Peaks that corresponded to molecules containing ^{13}C atoms or obvious impurities with anomalous mass defects were excluded from further analysis. The initial set of assigned peaks was used to refine the calibration of the m/z axis. If deviations were noticeable (greater than ±0.0005 m/z units), the axis was internally recalibrated with respect to the confidently assigned peaks, and the mass spectra were then reassigned with a lower tolerance of 0.00075 m/z. The vast majority of peaks corresponded to sodiated molecules (C$_c$H$_h$O$_o$N$_n$Na$^+$); protonated molecules (C$_c$H$_h$O$_o$N$_n$H$^+$) generally had small abundance. For the remainder of this paper, we discuss formulas for the corresponding neutral species, C$_c$H$_h$O$_o$N$_n$.

III. RESULTS AND DISCUSSION

Comparison of High-Resolution Mass Spectra of Unphotolyzed SOA Samples. High-resolution mass spectrometry (HR-MS) is a powerful tool for molecular characterization of SOA.[22] However, most of the results published so far have focused on SOA made from a limited number of precursors (limonene, α-pinene, isoprene, diesel fuel) and to filter extracts from a small number of field studies.[39−58] A database of HR mass spectra for laboratory-generated SOA is needed to help interpret HR-MS data for ambient aerosol samples. In this work, HR mass spectra of both natural and anthropogenic SOA are qualitatively compared to one another to identify the extent of similarity between them. We plan to follow up on this work with an extended compilation HR-MS data, and a more detailed comparison of the mass spectra.

Figures 2 and 3 compare mass spectra of all the fresh (unphotolyzed) SOA samples. The peak abundances are shown on a logarithmic scale; the same figures are reproduced in the Supporting Information section on a linear scale (Figures S1 and S2, respectively). The SOA produced by ozonolysis of monoterpenes APIN, BPIN, MYR, and LIM have qualitatively similar mass spectra (Figure 2) with a clear grouping of peaks into the monomeric (<300 Da), dimeric (300−500 Da) and larger oligomer groups. We refer to the molecules containing
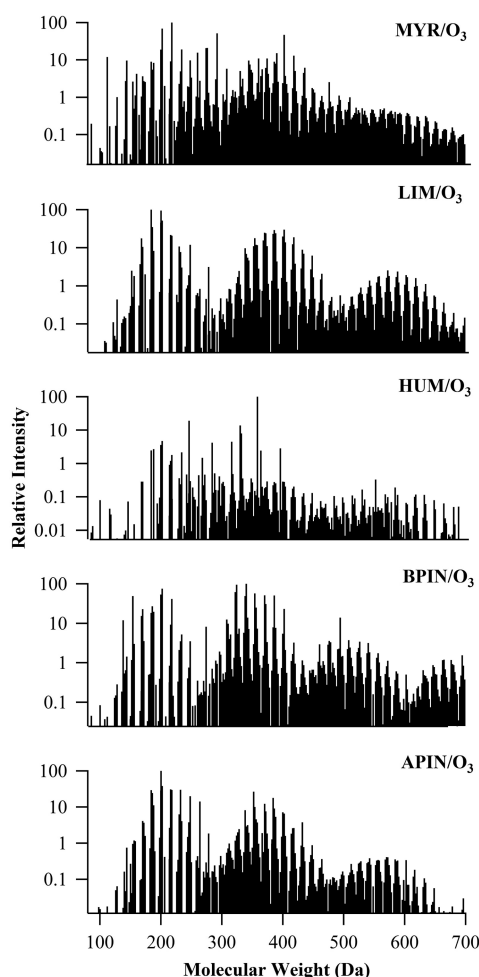
2597

dx.doi.org/10.1021/jp509476r | J. Phys. Chem. A 2015, 119, 2594−2606

Figure 2. Reconstructed mass spectra for all VOC/O$_3$ SOA samples (before photolysis) recorded in this work. The *x*-axis corresponds to the molecular weight of the neutral SOA compounds. The *y*-axis is on a log scale to make the weaker peaks of oligomeric compounds easier to see.

Figure 3. Reconstructed mass spectra for all VOC/NO$_x$ SOA samples (before photolysis) recorded in this work. The *x*-axis corresponds to the molecular weight of the neutral SOA compounds. The *y*-axis is on a log scale to make the weaker peaks of oligomeric compounds easier to see. Peaks in orange denote nitrogen-containing compounds.

two oxidized VOC molecules joined together as "dimers", three molecules joined together as "trimers", etc. The mass spectrum of HUM/O$_3$ SOA is qualitatively different, and appears to be dominated by a few monomeric products (this is especially obvious on the linear scale Figure S1). The mass spectra from OH/NO$_x$ photooxidation SOA samples display a greater level of diversity (Figure 3). The grouping of peaks into oligomeric species is still apparent for SOA from monoterpene precursors (e.g., APIN/NO$_x$, BPIN/NO$_x$, and MYR/NO$_x$ SOA) while mass spectra of SOA from sesquiterpene and aromatic precursors (e.g., HUM/NO$_x$, GUA/NO$_x$, and TMB/NO$_x$) are dominated by monomeric products.

The fraction of nitrogen-containing compounds (shown in orange in Figure 3) varies greatly between the SOA types; especially striking is the difference between the APIN/NO$_x$ and BPIN/NO$_x$ SOA. We note that organonitrates (ONs) produced under OH/NO$_x$ conditions may decompose by solvolysis reactions with water or methanol in the extracts before the HR-MS analysis. The SOA compounds remained in the methanol/water solutions for approximately 1 week prior to the HR-MS analysis, and although the solutions were frozen for most of that time, the solvolysis could potentially occur in ~2 h before freezing and after thawing. The solvolysis rates for most
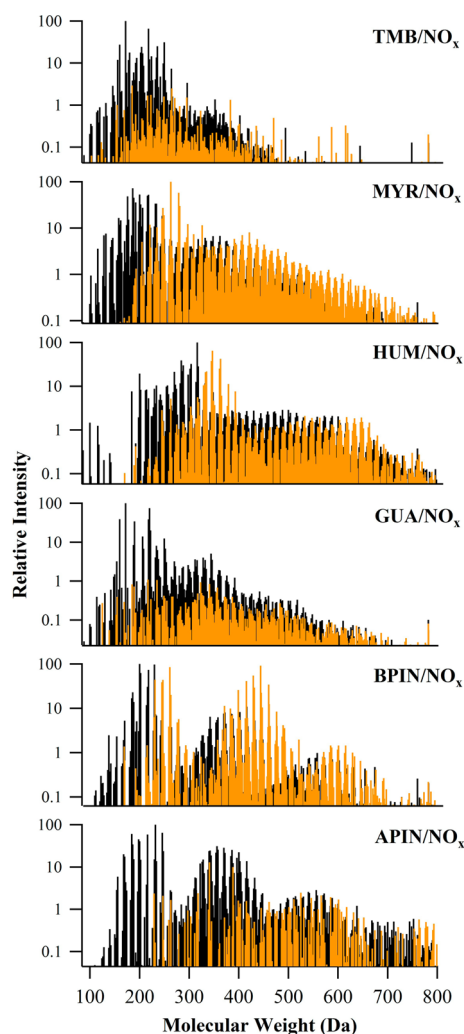
SOA compounds are not known but primary ONs are known to be more stable with respect to the solvolysis than tertiary ONs, and therefore more likely to survive in solution.[59,60] The fraction of primary ONs formed in BPIN (exocyclic double bond) oxidation should be higher than that in APIN (endocyclic double bond) oxidation, which may explain the higher fraction of the remaining ONs in the BPIN/NO$_x$ SOA extract.

Table 3 lists the most dominant peaks observed in each mass spectrum. In general, the major products tend to retain the carbon number of the precursor VOC. The monoterpenes (C$_{10}$H$_{16}$), humulene (C$_{15}$H$_{24}$), guaiacol (C$_7$H$_8$O$_2$), and trimethylbenzene (C$_9$H$_{12}$) produce for the most part C$_{10}$, C$_{15}$, C$_7$, and C$_9$ compounds, respectively. For example, a major peak appearing in the APIN/NO$_x$ and LIM/O$_3$ SOA is C$_{10}$H$_{16}$O$_3$, which can be assigned to pinonic acid, limononic acid and other isomers.[35,36,61] Compound C$_{10}$H$_{16}$O$_4$, presumably an isomer of hydroxy pinonic acid, is the most abundant peak in BPIN/NO$_x$ SOA. The C$_7$H$_8$O$_5$ compounds in GUA/NO$_x$ SOA may correspond to guaiacol with three more hydroxyl groups added to the ring.
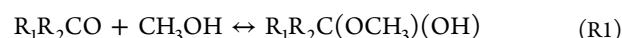
Table 3. Major Peaks Observed in the Mass Spectra for All Samples Analyzed in This Study

sample	neutral mass	chem formula[a]	relative intensities	
			before photolysis	after photolysis
APIN/NO$_x$	232.0576	C$_9$H$_{12}$O$_7$	100	100
	246.0892	C$_{14}$H$_{14}$O$_4$	65	66
	184.1094	C$_{10}$H$_{16}$O$_3$	61	78
BPIN/NO$_x$	200.1042	C$_{10}$H$_{16}$O$_4$	100	100
	230.1144	**C$_{11}$H$_{18}$O$_5$**	97	61
	444.2102	C$_{20}$H$_{32}$O$_9$	91	11
	202.1198	**C$_{10}$H$_{18}$O$_4$**	62	92
GUA/NO$_x$	172.0367	C$_7$H$_8$O$_5$	100	100
	220.0577	**C$_8$H$_{12}$O$_7$**	75	54
	160.0367	C$_6$H$_8$O$_5$	39	39
	218.0421	**C$_8$H$_{10}$O$_7$**	38	46
HUM/NO$_x$	316.1517	C$_{15}$H$_{24}$O$_7$	100	100
	347.1574	C$_{15}$H$_{25}$O$_8$N	65	35
	363.1523	C$_{15}$H$_{25}$O$_9$N	42	23
	304.1516	C$_{14}$H$_{24}$O$_7$	32	56
	284.1617	C$_{15}$H$_{24}$O$_5$	39	48
MYR/NO$_x$	263.0998	C$_{10}$H$_{17}$O$_7$N	100	64
	186.0886	C$_9$H$_{14}$O$_4$	72	100
	279.0947	C$_{10}$H$_{17}$O$_8$N	58	27
	188.0679	C$_8$H$_{12}$O$_5$	45	82
	176.0679	C$_7$H$_{12}$O$_5$	49	77
TMB/NO$_x$	172.0367	C$_7$H$_8$O$_5$	100	100
	218.0784	C$_9$H$_{14}$O$_6$	66	93
	250.1044	**C$_{10}$H$_{18}$O$_7$**	31	60
APIN/O$_3$	200.1407	**C$_{11}$H$_{20}$O$_3$**	100	100
	202.1199	**C$_{10}$H$_{18}$O$_4$**	38	46
	216.1355	**C$_{11}$H$_{20}$O$_4$**	31	23
	186.1251	**C$_{10}$H$_{18}$O$_3$**	24	41
BPIN/O$_3$	340.2241	**C$_{19}$H$_{32}$O$_5$**	100	100
	324.1928	C$_{18}$H$_{28}$O$_5$	95	55
	202.1199	**C$_{10}$H$_{18}$O$_4$**	75	89
	154.0989	C$_9$H$_{14}$O$_2$	49	64
HUM/O$_3$	358.3075	C$_{21}$H$_{42}$O$_4$	100	100
	246.146	C$_{12}$H$_{22}$O$_5$	19	33
	330.2765	C$_{19}$H$_{38}$O$_4$	14	13
LIM/O$_3$	184.1094	C$_{10}$H$_{16}$O$_3$	100	78
	200.1407	**C$_{11}$H$_{20}$O$_3$**	95	100
	202.1199	**C$_{10}$H$_{18}$O$_4$**	52	76
MYR/O$_3$	218.1148	**C$_{10}$H$_{18}$O$_5$**	100	100
	202.1199	**C$_{10}$H$_{18}$O$_4$**	69	85
	292.1517	C$_{13}$H$_{24}$O$_7$	51	40

[a]Formulas that are in bold text likely correspond to hemiacetals formed through reaction R1 with methanol. The formulas of the original SOA compounds can be obtained from the hemiacetal formulas by subtracting CH$_4$O.

However, there are many interesting deviations from the general trend of conserving the starting VOC precursor carbon number. For example, while the strongest peaks in HUM/NO$_x$ SOA have 15 or 14 C atoms (C$_{15}$H$_{24}$O$_7$, C$_{15}$H$_{25}$O$_8$N, C$_{15}$H$_{25}$O$_9$N, C$_{14}$H$_{24}$O$_7$ and C$_{15}$H$_{24}$O$_5$), the largest peak in HUM/O$_3$ SOA, namely C$_{21}$H$_{42}$O$_4$, appears to have little in common with the starting VOC precursor formula. It is likely a reaction product of a C$_{15}$ and a C$_6$ product of humulene ozonolysis. The major peaks in BPIN/NO$_x$ SOA (C$_{20}$H$_{32}$O$_9$) and in BPIN/O$_3$ SOA (C$_{19}$H$_{32}$O$_5$) correspond to dimeric compounds in contrast to other SOA, in which monomeric compounds prevail.

The occurrence of major C$_{11}$ compounds in SOA from monoterpenes, C$_8$ compounds in GUA/NO$_x$ SOA, and C$_{10}$ compounds in TMB/NO$_x$ (Table 3) can be explained by hemiacetal R1 and/or ester R2 formation reactions between the SOA compounds and methanol as previously observed by Bateman et al.[31]

$$R_1R_2CO + CH_3OH \leftrightarrow R_1R_2C(OCH_3)(OH) \quad (R1)$$

$$RC(O)OH + CH_3OH \leftrightarrow RC(O)OCH_3 + H_2O \quad (R2)$$

Bateman et al. showed that reaction R1 quickly reaches equilibrium in methanol solutions, and is more significant for aldehydes than for ketones, while reaction R2 is kinetically constrained. The hemiacetals produced in the 70/30 v/v % methanol/water solution should contain one additional carbon atom compared to their SOA carbonyl precursors. For example, the C$_{11}$H$_{20}$O$_3$ compound, which appears as one of the major peaks in APIN/O$_3$ and LIM/O$_3$ SOA is a hemiacetal of C$_{10}$H$_{16}$O$_2$ (pinonaldehyde or limononaldehyde) and methanol.[31] The C$_{11}$H$_{18}$O$_5$ compound in BPIN/NOx is presumably a hemiacetal corresponding to C$_{10}$H$_{14}$O$_4$. Likewise, the C$_{11}$H$_{18}$O$_4$ compound observed in the APIN/O$_3$, BPIN/O$_3$, LIM/O$_3$, and MYR/O$_3$ samples must be a hemiacetal corresponding to C$_{10}$H$_{14}$O$_3$ (it would otherwise be challenging to explain why a major product of a monoterpene oxidation should have a formula C$_{11}$H$_{19}$O$_4$ corresponding to a decandedioic acid isomer). The TMB/NO$_x$ compound C$_{10}$H$_{18}$O$_7$ is conceivably a hemiacetal of C$_9$H$_{14}$O$_6$ (the latter is also observed as a major species in TMB/NO$_x$). The compounds C$_8$H$_{10}$O$_7$ and C$_8$H$_{12}$O$_7$ in GUA/NO$_x$ SOA could also be products of reactions R1 or R2. As mentioned in the experimental section, the hemiacetal formation is not expected to drastically affect photochemical properties of SOA relative to pure water solutions.

We evaluated the extent of overlap between the exact m/z values reported between all the OH/NO$_x$ and O$_3$ SOA samples examined in this work (Table 4). For both sets of oxidation conditions, close to 50% of the assigned peaks are unique to a

Table 4. Overlap of Peaks between VOC/NO$_x$ Samples and VOC/O$_3$ Samples

SOA class[a]	All VOC/NO$_x$ SOA	subset of APIN/NO$_x$, BPIN/NO$_x$, HUM/NO$_x$, MYR/NO$_x$	all VOC/O$_3$ SOA	subset of APIN/O$_3$, BPIN/O$_3$, HUM/O$_3$, MYR/O$_3$
total peaks assigned	4178	3005	1474	1379
peaks unique to a specific VOC precursor	2427 (58.1%)	1722 (57.3%)	653 (44.3%)	755 (54.7%)
peaks observed from more than one precursor	1741 (41.7%)	1150 (38.3%)	638 (43.3%)	436 (31.6%)
peaks that appear in all samples	10 (0.2%)	133 (4.4%)	183 (12.4%)	188 (13.6%)

[a]The analysis is carried out for all of the VOC/NO$_x$ SOA and VOC/O$_3$ SOA examined in this work. An analysis of a subset of data with four overlapping VOC precursors (APIN, BPIN, HUM, MYR) is also included for comparison.

specific precursor. Furthermore, the fraction of peaks appearing in all samples produced under the same oxidation conditions is relatively low, especially for the subset of OH/NO$_x$ SOA. Since we used only terpenes in the O$_3$ experiments and both terpene and aromatic precursors in the OH/NO$_x$ experiments, we also calculated the extent of the peak overlap for a smaller subset of SOA made from four terpene precursors APIN, BPIN, HUM, and MYR. The fractions of unique peaks remained significant and the fraction of peaks appearing in all samples produced under the same oxidation conditions remained relatively low even for this subset of closely related precursors. These observations suggest that HR-MS could potentially be used to distinguish SOA made from different VOC precursors based on the distribution of peaks in the mass spectra. In the future, we plan to use Principal Component Analysis (PCA) to estimate the atmospheric contribution for each type of SOA created in this study.

However, it will not be possible to unambiguously attribute SOA to a specific set of precursors and oxidants using only the information on the major peaks appearing in the direct-infusion ESI mass spectra (Table 3). Coupling to LC methods would be required to remove some of the ambiguity. For example, one of the molecular formulas appearing in all the O$_3$ samples is C$_{10}$H$_{16}$O$_3$, which could correspond to pinonic acid, but could also be limononic acid or any of the keto-acids produced from monoterpenes.[62] Another molecular formula, C$_9$H$_{14}$O$_3$, identified as ketolimononaldehyde in limonene SOA,[63] is also appearing in all the O$_3$ samples. Other common formulas observed in all O$_3$ and all OH/NO$_x$ samples include C$_{10}$H$_{14}$O$_5$, possibly peroxo-pinic acid or its isomer,[64] previously observed in α-pinene ozonolysis as well as campholenic aldehyde ozonolysis,[65] and C$_{10}$H$_{16}$O$_6$, which has been potentially identified as an ester of glutaric acid or 5-hydroxy-pentanoic acid as seen in the study of ozonolysis of cyclohexene by Hamilton et al.[66] A study of the ozonolysis of α-pinene and limonene by Warscheid and Hoffmann[67] also identified the molecular formula of C$_{10}$H$_{16}$O$_6$ through an online MS^n technique. Their analysis showed two structurally different carboxylic acid species - a hydroxyl-acidic ester as well as a peroxyacetyl carboxylic acid. It is also of interest that one recurring molecular formula in all OH/NO$_x$ samples is that of C$_9$H$_{13}$O$_7$N. Assuming that it is a nitric acid ester (ROH + HONO$_2$ → RONO$_2$ + H$_2$O), the unesterified compound would have the formula C$_9$H$_{14}$O$_5$, a compound observed in APIN, BPIN, HUM, MYR, and TMB OH/NO$_x$ samples in this study as well as in ozonolysis of alpha-pinene,[68] limonene,[69,70] campholenic aldehyde[65] in previous studies. It is not clear how the C$_9$H$_{13}$O$_7$N could be formed from the aromatic precursors; however, we cannot exclude the possibility that its occurrence in all samples is an experimental artifact from "carry-over" between SOA generated from different precursors on different days.

Effect of Photolysis on SOA Composition. Figure 4 shows representative high-resolution mass spectra of APIN SOA samples before and after 1 h of photolysis. Figure S3 in the Supporting Information section shows similar plots for the rest of the SOA investigated here. The mass spectra noticeably change after irradiation, especially in the dimeric (300−500 m/z) and trimeric (500−700 m/z) regions. The higher molecular weight (MW) compounds appear to be converted to lower molecular weight species by photolysis with an accompanying shift in the distribution of relative intensity toward lower-MW compounds.
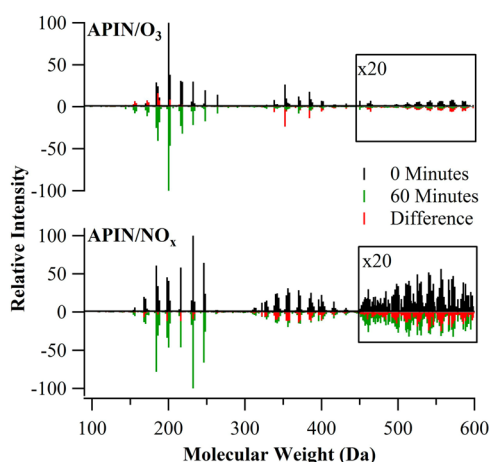

Figure 4. Mass spectra of APIN/O$_3$ and APIN/NO$_x$ SOA solutions before (black) and after (green) 1 h of photolysis. The mass spectra after photolysis are inverted for clarity. The difference (red, after − before) is representative of the change that occurred during the photolysis time.

The average atom numbers (C, H, O, N) and average elemental ratios (H/C, O/C, and N/C) can be extracted from the assigned molecular formulas C$_c$H$_h$O$_o$N$_n$. These average quantities were used to assess the extent in the photolysis-induced overall change in SOA composition. The ratio O/C indicates the degree of oxidation, while H/C is a good indicator of the degree of unsaturation in SOA molecules. All averaged quantities were weighted with respect to the relative intensity (I), for all assigned compounds, indexed with i.

$$\langle X \rangle = \frac{\sum I_i x_i}{\sum I_i} \quad (x = c,\, o,\, h,\, n,\, \text{or DBE}) \tag{3}$$

$$\langle X/Y \rangle = \frac{\sum I_i x_i}{\sum I_i y_i} = \frac{\langle X \rangle}{\langle Y \rangle} \quad (x,\, y = o,\, h,\, \text{or } n) \tag{4}$$

Table 5 summarizes the analysis results. The table also shows the average double bond equivalent (DBE) value, also known as degree of unsaturation to organic chemists.[71] Average DBE is calculated by,

$$\langle \text{DBE}_{\text{uncorrected}} \rangle = 1 - \frac{\langle h \rangle}{2} + \frac{\langle n \rangle}{2} + \langle c \rangle \tag{5}$$

and represents the total number of double bonds and rings in a molecule. Since most of the N-containing compounds in SOA are expected to be either nitrocompounds (-NO$_2$) or nitric acid esters (-ONO$_2$), the true DBE is higher than that predicted by eq 5 by the average number of nitrogen atoms:

$$\langle \text{DBE}_{\text{corrected}} \rangle = 1 - \frac{\langle h \rangle}{2} + \frac{3\langle n \rangle}{2} + \langle c \rangle$$

$$= \langle \text{DBE}_{\text{uncorrected}} \rangle + \langle n \rangle \tag{6}$$

Some of the SOA examined in this work have higher DBE values than one would have expected based on the known oxidation mechanisms of VOCs. For example, the APIN/NO$_x$ SOA has an average formula C$_{16.6}$H$_{22.7}$O$_{6.2}$N$_{0.067}$ and an uncorrected DBE of 6.3 and. One could potentially explain such high DBE value if all the oxygen atoms in APIN/NO$_x$ SOA compounds were tied in carbonyls groups but this scenario is unlikely. It is more reasonable to assume that a large

Table 5. Average Molecular Formulas, Double Bond Equivalents (DBE), and Average Atomic Ratios X/C, where X is O, H, or N, before and after 1 h of Photolysis of SOA Solutions

reacn	av mol formula		$\langle DBE \rangle^d$		$\langle O/C \rangle$		$\langle H/C \rangle$		$\langle N/C \rangle$	
	before photolysis (0 min)	after photolysis (60 min)	0 min	60 min	0 min	60 min	0 min	60 min	0 min	60 min
APIN/NO$_x$	$C_{16.6}H_{22.7}O_{6.2}N_{0.067}$	$C_{15.4}H_{21.0}O_{5.8}N_{0.075}$	6.28	5.93	0.373	0.377	1.42	1.36	0.00403	0.00487
BPIN/NO$_x$	$C_{15.5}H_{25.4}O_{6.9}N_{0.063}$	$C_{14.6}H_{23.8}O_{6.1}N_{0.043}$	3.83	3.72	0.445	0.418	1.64	1.63	0.00406	0.00295
GUA/NO$_x$	$C_{9.90}H_{12.7}O_{7.4}N_{0.081}$	$C_{9.90}H_{12.8}O_{7.4}N_{0.075}$	4.59	4.54	0.747	0.747	1.28	1.29	0.00818	0.00758
HUM/NO$_x$	$C_{17.5}H_{28.4}O_{8.2}N_{0.38}$	$C_{17.5}H_{28.5}O_{7.9}N_{0.21}$	4.49	4.15	0.469	0.451	1.62	1.63	0.0217	0.0120
MYR/NO$_x$	$C_{12.6}H_{20.4}O_{8.0}N_{0.48}$	$C_{12.0}H_{19.3}O_{7.5}N_{0.28}$	3.64	3.49	0.635	0.625	1.62	1.61	0.0381	0.0233
TMB/NO$_x$	$C_{9.21}H_{11.8}O_{6.0}N_{0.082}$	$C_{9.08}H_{13.2}O_{6.1}N_{0.063}$	3.85	3.51	0.651	0.672	1.39	1.45	0.00890	0.00694
APIN/O$_3$	$C_{14.0}H_{23.7}O_{5.1}$	$C_{11.9}H_{20.5}O_{4.4}$	3.15	2.65	0..364	0.370	1.69	1.72		
BPIN/O$_3$	$C_{17.4}H_{28.4}O_{5.5}$	$C_{16.2}H_{26.6}O_{5.3}$	4.20	3.90	0.316	0.327	1.63	1.64		
HUM/O$_3$	$C_{18.0}H_{34.1}O_{4.9}$	$C_{16.8}H_{32.0}O_{4.5}$	1.95	1.80	0.272	0.268	1.89	1.90		
LIM/O$_3$	$C_{16.5}H_{27.4}O_{6.4}$	$C_{14.4}H_{24.1}O_{5.5}$	3.80	3.35	0.388	0.382	1.66	1.67		
MYR/O$_3$	$C_{14.4}H_{24.8}O_{6.7}$	$C_{12.9}H_{22.2}O_{5.9}$	3.00	2.80	0.465	0.457	1.72	1.72		
LIM/O$_3^a$	$C_{14}H_{22}O_{7.0}$	$C_{12}H_{18}O_{6.4}$	4.00	4.00	0.500	0.533	1.57	1.50		
ISO/NO$_x^b$	$C_{12}H_{19}O_9N_{0.08}$	$C_{10}H_{16}O_8N_{0.40}$	3.54	3.20	0.750	0.800	1.58	1.60	0.00667	0.0400
NAP/NO$_x^c$	$C_{14.1}H_{14.5}O_{5.1}N_{0.08}$	$C_{11.8}H_{14.9}O_{4.5}N_{0.02}$	7.89	5.36	0.362	0.381	1.03	1.26	0.00567	0.00169

^{a}Bateman et al.;[15] 24 h photolysis, different light source. ^{b}Nguyen et al.;[19] 4 h photolysis, different light source. ^{c}Lee et al.;[20] 4 h photolysis, different light source. ^{d}Uncorrected DBE from eq 5. Corrected values can be easily calculated from eq 6.

fraction of SOA products contain intramolecular cycles that contribute to the high observed DBE values.

Degradation of oligomeric compounds seen in the mass spectra appears to be a common result for aqueous direct photolysis of the SOA, regardless of the VOC precursor and oxidation conditions leading to SOA. We note that photolysis-driven formation of lower molecular weight compounds is well-known in the photochemistry of dissolved organic matter (DOM) but is much less studied in the case of SOA.[72−74] Although the effect of photolysis on the molecular size is modest, the photolysis time used in these experiments is only 1 h, and the effect can be expected to be stronger for longer photolysis durations. For example, Nguyen et al. saw no evidence of photodegradation stopping after 0, 1, 2, 3, and 4 h of the aqueous photolysis of isoprene/NO$_x$ SOA.[19] Using actinometry to estimate the photon flux from the lamp used in experiments, we have concluded that 1 h of photolysis under our lamp is approximately equivalent to ∼4 h of photolysis under the overhead sun in the case of GUA/NO$_x$ SOA and ∼8 h in the case of APIN/O$_3$ SOA. The lifetime of droplets in cumulus clouds is typically in the range of 10−40 min, so the times probed here correspond to photolysis that may be experienced during several cloud cycles.[75] In this work we opted to fix the photolysis time and vary the type of SOA, assuming that the extent of photodegradation would scale with photolysis time (doing time-dependent studies for all of the SOA listed in Table 1 would be prohibitively time-consuming).

One possible explanation for the reduction in the average number of carbon atoms during photolysis is the photochemistry that occurs with organic molecules that contain a peroxy group. Organic peroxides are known to be abundant in SOA produced by ozonolysis of alkenes. For example, Docherty et al. estimate that a large fraction of compounds in APIN/O$_3$ and BPIN/O$_3$ SOA are peroxides.[76] Peroxides are well-known[2] to undergo direct photolysis by breaking the O−O bond in the molecule:

$$RCH_2OOR' \xrightarrow{h\nu} RCH_2O^\bullet + R'O^\bullet \rightarrow RC(O)H + R'OH$$
(R3)
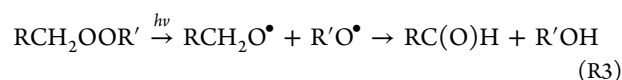
The photolysis quantum yield is known to be high in water,[77] and the resulting free radicals do not recombine but rather disproportionate leading to carbonyl and alcohol products, as shown in the reaction R3 example.[78] Even if these free radicals manage to escape from the solvent cage, secondary reactions would generally result in smaller products relative to the size of the precursor peroxide compound, which would consequentially also reduce the average C value.

Photochemistry of carbonyls also likely contributes to the reduction in the average C-number. In Norrish type-I splitting, carbonyl groups undergo α-cleavage that produces peroxy radicals in the presence of dissolved oxygen.[79]

$$R'C(O)R \xrightarrow{h\nu, O_2} R'C(O)OO^\bullet + ROO^\bullet \rightarrow secondary\ products$$
(R4)
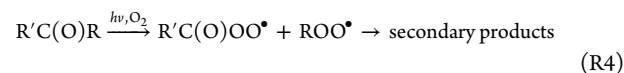
Secondary reactions of peroxy radicals produce carbonyls, alcohols, and carboxylic acids as stable products.[80,81] While Norrish type-I splitting is the predominant path for small carbonyls (C$_1$−C$_5$), Norrish type-II splitting is favored by the larger carbonyls. Norrish type-II splitting cleaves the molecule into a smaller alkene and a carbonyl:

$$R'C(O)CH_2CH_2CH_2R \xrightarrow{h\nu} R'C(O)CH_3 + CH_2{=}CHR$$
(R5)
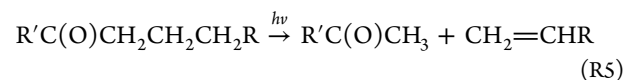
The resulting carbonyl products can then be further photolyzed by the Norrish type-I and type-II mechanisms to produce even smaller products.[82] These processes can be efficient in water as demonstrated by Norrish type-II photoisomerization of *cis*-pinonic acid into limononic acid occurring with a quantum yield of about 0.5.[32]

Neither photolysis of peroxides nor photolysis of carbonyls provides an explanation for the observed reduction in the average DBE. For example, photolysis of peroxides converts a peroxide (DBE contribution = 0) into an alcohol (DBE contribution = 0) and a carbonyl (DBE contribution = 1), thus increasing the average DBE. Likewise, Norrish type-II splitting converts a carbonyl (DBE contribution = 1) into another carbonyl and alkene (DBE contribution = 1 each), leaving the average DBE unchanged. It is possible that the observed decrease in DBE is in fact an artifact of ESI, which tends to
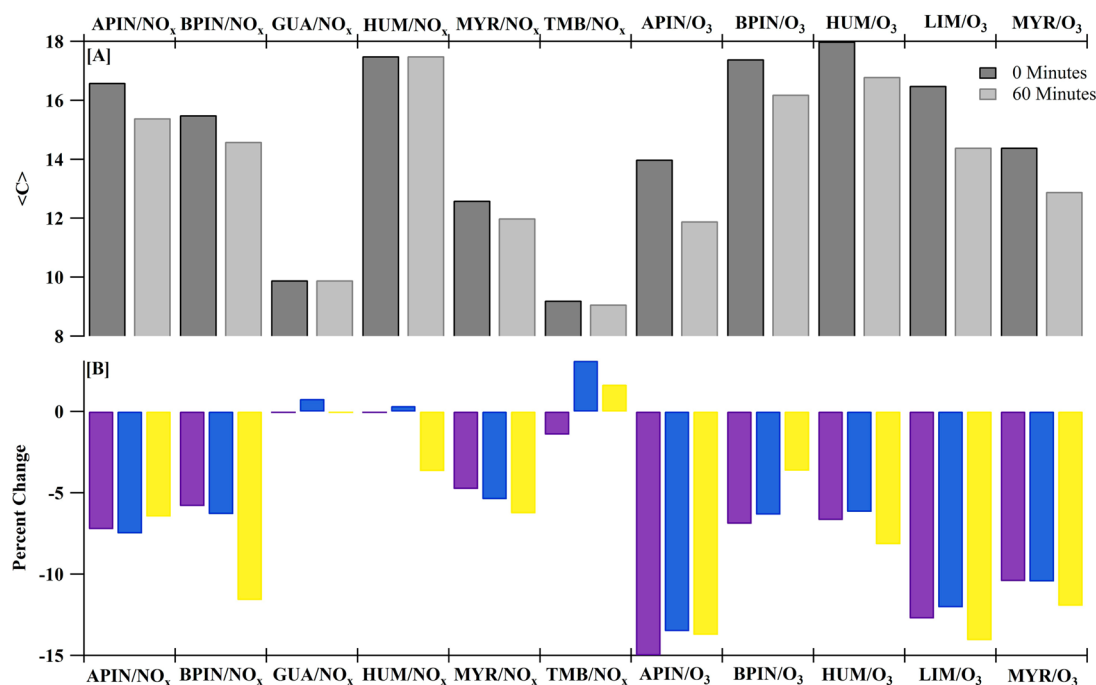
Figure 5. Panel A shows the average number of carbon atoms per molecule before (dark gray bars) and after (light gray bars) 1 h of photolysis. Panel B shows the percent change, $[(\text{after} - \text{before})/\text{before}] \times 100$, in the average number of C (purple), H (blue), and O (yellow) atoms following the 1 h of photolysis.

detect larger compounds with higher sensitivity.[83] The smaller photolysis products have suppressed intensities in the mass spectrum and therefore contribute less than they should to the average DBE. As DBE in SOA generally increases with molecular size,[35] the reduction of ESI sensitivity with molecular size would produce an artificial reduction in the apparent DBE. We note that the same effect makes the decrease in C underestimated because the precursor molecules are detected with higher sensitivity than their smaller photolysis products.

In this study, very little change is observed with regard to the average H/C and O/C ratios before and after photolysis (Table 5). This is an important observation as H/C and O/C are routinely measured in field studies as an indicator of SOA oxygenation or aging.[84−86] Results of this study indicate that tracking the average H/C and O/C ratios may miss important photochemical aging processes such as photodegradation. The changes in the molecular level composition of SOA induced by aqueous photolysis are observable; however, the average atomic ratios hardly change in the process. Furthermore, the reduction in the number of C atoms in SOA compounds with constant O/C ratio may affect the volatility of the photochemically aged aerosols. As a result, the particles are likely to lose some of their mass after exposure to solar radiation.

On the other hand, for SOA that is formed in the presence of NO_x, the average N/C ratio goes down significantly with photolysis. This reduction in N/C is likely attributed to the photolysis of organonitrates

$$RONO_2 \xrightarrow{h\nu} RO^\bullet + NO_2 \tag{R6}$$

with secondary processes forming stable nitrogen-free compounds from RO radicals. This significant decrease in the N/C ratio is different from the trend observed in direct aqueous photolysis of isoprene/NO_x SOA where the number of nitrogen-containing compounds increased substantially during photolysis.[19] This suggests that nitrogen-containing molecules

in isoprene SOA may be a unique case that may require further investigation. Our results indicate that for a majority of SOA, the N/C ratio is an additional useful indicator of aerosol age, complementary to the commonly used O/C ratio.

Figure 5 shows the percent change in the average number of C, H, and O atoms in SOA molecules following 1 h photolysis. This figure indicates that the extent of photolysis-driven change is generally larger for ozone-generated SOA than for OH/NO_x photooxidation SOA. The ozone-generated SOA were produced in the dark, and the first time these compounds encountered radiation was after they were extracted from the filter. In contrast, the OH/NO_x SOA were already irradiated by the 310 nm light while they were being formed in the chamber. This gave the most photolyzable SOA compounds a chance to photolyze in the airborne particles before collection of the SOA sample and its subsequent photolysis in solution. We can extrapolate this result by predicting that SOA produced during the night, with O_3 and NO_3 serving as oxidants, should be more photolabile than SOA formed during the day time, with OH serving as the oxidant. Our ongoing experiments are testing this hypothesis by comparing photochemistry of SOA generated in the dark by NO_3 oxidation with the photochemistry of OH/NO_x-generated SOA.

Figure 5 additionally suggests that the role of direct photolysis is substantially smaller for SOA made from aromatic precursors (TMB and GUA), as evidenced by the much smaller change in C compared to SOA from nonaromatic precursors. The aromatic compounds are known to largely retain their carbon number during photolysis. For example, in the direct aqueous photolysis of 2-nitrophenol,[87] the major photoproducts catechol, nitrohydroquinone, 3-nitrocatechol, and 2-nitrosophenol retain the aromatic ring. It has also been previously shown that nitrocompounds photodegrade fairly slowly in aqueous solutions.[88] In an oxygen-depleted environment, aromatic nitrocompounds can undergo rapid one-

electron photochemical reduction. However, in the presence of oxygen (under the experimental conditions of this work), this reaction is completely quenched. The photostability of these compounds is attributed to the charge-transfer character of their triplet states. Consequently, the quantum yield of direct photolysis of these compounds in water is quite low ($\phi \sim 10^{-5}$).[87−89]

IV. CONCLUSION

We examined the effect of UV irradiation on the high-resolution mass spectra of water/methanol solutions of several representative types of SOA produced from biogenic and anthropogenic precursors by OH/NO$_x$ or O$_3$ oxidation. A comparison of the mass spectra taken before and after irradiation showed that SOA compounds, especially the oligomeric ones, photodegrade in solution on atmospherically relevant time scales. Peroxides, carbonyls, organonitrates, and nitroaromatic compounds likely contribute to photodegradation. The extent of the photodegradation is not correlated with the absorption coefficient; the SOA prepared from aromatic precursors appear to be more resilient to photodegradation despite being more absorbing than SOA prepared from monoterpenes. The irradiation tends to reduce the average size (carbon number) of SOA compounds. However, the average atomic ratios O/C and H/C do not change significantly suggesting that this type of photochemical aging would be missed by methods relying on measurements of the average composition instead of detailed molecular characterization. These findings have important implications for understanding the aging chemistry of atmospheric aerosols during their cloud processing cycles.

We also compared high-resolution mass spectra of unphotolyzed SOA in an effort to gauge the extent of similarity between the mass spectra. Many major peaks found in the mass spectra are not specific to their VOC precursors because they are observed in mass spectra of different types of SOA. However, a number of smaller unique peaks are also detected in the mass spectra. Our qualitative comparison suggests that it should be possible to attribute different types of SOA to a specific VOC precursor and/or specific set of oxidation conditions based on the occurrence of sets of unique peaks in the high-resolution mass spectra. This study is a step toward building a reference library of high-resolution mass spectra for laboratory-generated SOA to aid in the assignments of field data collected by the same method. Future efforts should focus on principal component analysis of large libraries of high-resolution mass spectra collected by different groups.

ASSOCIATED CONTENT

Ⓢ Supporting Information

Figures showing linear-scale versions of Figures 2 and 3 and a comparison of mass spectra before and after photolysis for all the SOA samples examined in this work. This material is available free of charge via the Internet at http://pubs.acs.org.

AUTHOR INFORMATION

Corresponding Author
*Tel.: 949-824-1262. E-mail: nizkorod@uci.edu.

Notes
The authors declare no competing financial interest.

REFERENCES

(1) Solomon, S.; Qin, D.; Manning, M.; Chen, Z.; Marquis, M.; Averyt, K.; Tignor, M.; Miller, H. *IPCC Climate Change 2007: The Physical Science Basis*; Cambridge University Press: Cambridge, U.K., 2007.

(2) Finlayson-Pitts, B. J.; Pitts J. N., Jr. *Chemistry of the Upper and Lower Atmosphere: Theory, Experiments, and Applications*; Academic Press: San Diego, CA, USA, 2000.

(3) Pankow, J. F. An Absorption Model of the Gas/Aerosol Partitioning Involved in the Formation of Secondary Organic Aerosol. *Atmos. Environ.* **1994**, *28*, 189−193.

(4) Odum, J. R.; Hoffmann, T.; Bowman, F.; Collins, D.; Flagan, R. C.; Seinfeld, J. H. Gas/Particle Partitioning and Secondary Organic Aerosol Yields. *Environ. Sci. Technol.* **1996**, *30*, 2580−2585.

(5) Monge, M. E.; Rosenorn, T.; Favez, O.; Muller, M.; Adler, G.; Abo Riziq, A.; Rudich, Y.; Herrmann, H.; George, C.; D'Anna, B. Alternative Pathway for Atmospheric Particles Growth. *Proc. Natl. Acad. Sci. U. S. A.* **2012**, *109*, 6840−6844.

(6) Koppmann, R. *Volatile Organic Compounds in the Atmosphere*; Blackwell: Oxford, U.K., 2008; 512 pp.

(7) Ervens, B.; Turpin, B.; Weber, R. Secondary Organic Aerosol Formation in Cloud Droplets and Aqueous Particles (AqSOA): A Review of Laboratory, Field and Model Studies. *Atmos. Chem. Phys.* **2011**, *11*, 11069−11102.

(8) Atkinson, R.; Baulch, D. L.; Cox, R. A.; Crowley, J. N.; Hampson, R. F.; Hynes, R. G.; Jenkin, M. E.; Kerr, J. A.; Rossi, M. J.; Troe, J. Evaluated Kinetic and Photochemical Data for Atmospheric Chemistry: Supplement VI—IUPAC Subcommittee on Gas Kinetic Data Evaluation for Atmospheric Chemistry. *J. Phys. Chem. Ref. Data* **1997**, *26*, 1329−1499.

(9) Griffin, R. J.; Cocker, D. R.; Flagan, R. C.; Seinfeld, J. H. Organic Aerosol Formation from the Oxidation of Biogenic Hydrocarbons. *J. Geophys. Res. Atmos.* **1999**, *104*, 3555−3567.

(10) Albinet, A.; Minero, C.; Vione, D. Photochemical Generation of Reactive Species Upon Irradiation of Rainwater: Negligible Photoactivity of Dissolved Organic Matter. *Sci. Total Environ.* **2010**, *408*, 3367−3373.

(11) Wang, Y.; Arellanes, C.; Curtis, D. B.; Paulson, S. E. Probing the Source of Hydrogen Peroxide Associated with Coarse Mode Aerosol Particles in Southern California. *Environ. Sci. Technol.* **2010**, *44*, 4070−4075.

(12) Lim, Y.; Tan, Y.; Perri, M.; Seitzinger, S.; Turpin, B. Aqueous Chemistry and Its Role in Secondary Organic Aerosol (SOA) Formation. *Atmos. Chem. Phys.* **2010**, *10*, 10521−10539.

(13) Perri, M. J.; Seitzinger, S.; Turpin, B. J. Secondary Organic Aerosol Production from Aqueous Photooxidation of Glycolaldehyde: Laboratory Experiments. *Atmos. Environ.* **2009**, *43*, 1487−1497.

(14) Tan, Y.; Carlton, A. G.; Seitzinger, S. P.; Turpin, B. J. SOA from Methylglyoxal in Clouds and Wet Aerosols: Measurement and Prediction of Key Products. *Atmos. Environ.* **2010**, *44*, 5218−5226.

(15) Bateman, A. P.; Nizkorodov, S. A.; Laskin, J.; Laskin, A. Photolytic Processing of Secondary Organic Aerosols Dissolved in Cloud Droplets. *Phys. Chem. Chem. Phys.* **2011**, *13*, 12199–12212.

(16) Reed Harris, A. E.; Ervens, B.; Shoemaker, R. K.; Kroll, J. A.; Rapf, R. J.; Griffith, E. C.; Monod, A.; Vaida, V. Photochemical Kinetics of Pyruvic Acid in Aqueous Solution. *J. Phys. Chem. A* **2014**, *188*, 8505–8516.

(17) Guzman, M.; Colussi, A.; Hoffmann, M. Photoinduced Oligomerization of Aqueous Pyruvic Acid. *J. Phys. Chem. A* **2006**, *110*, 3619–3626.

(18) Rincón, A. G.; Guzmán, M. I.; Hoffmann, M.; Colussi, A. Thermochromism of Model Organic Aerosol Matter. *J. Phys. Chem. Lett.* **2009**, *1*, 368–373.

(19) Nguyen, T. B.; Laskin, A.; Laskin, J.; Nizkorodov, S. A. Direct Aqueous Photochemistry of Isoprene High-NOx Secondary Organic Aerosol. *Phys. Chem. Chem. Phys.* **2012**, *14*, 9702–9714.

(20) Lee, H. J.; Aiona, P. K.; Laskin, A.; Laskin, J.; Nizkorodov, S. A. Effect of Solar Radiation on the Optical Properties and Molecular Composition of Laboratory Proxies of Atmospheric Brown Carbon. *Environ. Sci. Technol.* **2014**, *48*, 10217–10226.

(21) Epstein, S. A.; Nizkorodov, S. A. A Comparison of the Chemical Sinks of Atmospheric Organics in the Gas and Aqueous Phase. *Atmos. Chem. Phys. Discuss.* **2012**, *12*, 10015–10058.

(22) Nizkorodov, S. A.; Laskin, J.; Laskin, A. Molecular Chemistry of Organic Aerosols through the Application of High Resolution Mass Spectrometry. *Phys. Chem. Chem. Phys.* **2011**, *13*, 3612–3629.

(23) Geron, C.; Rasmussen, R.; Arnts, R.; Guenther, A. A Review and Synthesis of Monoterpene Speciation from Forests in the United States. *Atmos. Environ.* **2000**, *34*, 1761–1781.

(24) Kim, Y. M.; Harrad, S.; Harrison, R. M. Concentrations and Sources of VOCs in Urban Domestic and Public Microenvironments. *Environ. Sci. Technol.* **2001**, *35*, 997–1004.

(25) McDonald, J. D.; Zielinska, B.; Fujita, E. M.; Sagebiel, J. C.; Chow, J. C.; Watson, J. G. Fine Particle and Gaseous Emission Rates from Residential Wood Combustion. *Environ. Sci. Technol.* **2000**, *34*, 2080–2091.

(26) Bones, D. L.; Henricksen, D. K.; Mang, S. A.; Gonsior, M.; Bateman, A. P.; Nguyen, T. B.; Cooper, W. J.; Nizkorodov, S. A. Appearance of Strong Absorbers and Fluorophores in Limonene-O_3 Secondary Organic Aerosol Due to NH_4^+-Mediated Chemical Aging over Long Time Scales. *J. Geophys. Res.: Atmos.* **2010**, DOI: 10.1029/2009JD012864.

(27) Matsumoto, K.; Kawai, S.; Igawa, M. Dominant Factors Controlling Concentrations of Aldehydes in Rain, Fog, Dew Water, and in the Gas Phase. *Atmos. Environ.* **2005**, *39*, 7321–7329.

(28) Munger, J. W.; Collett, J., Jr.; Daube, B., Jr.; Hoffmann, M. R. Fogwater Chemistry at Riverside, California. *Atmos. Environ., Part B* **1990**, *24*, 185–205.

(29) Volkamer, R.; Ziemann, P.; Molina, M. Secondary Organic Aerosol Formation from Acetylene (C_2H_2): Seed Effect on SOA Yields Due to Organic Photochemistry in the Aerosol Aqueous Phase. *Atmos. Chem. Phys.* **2009**, *9*, 1907–1928.

(30) Updyke, K. M.; Nguyen, T. B.; Nizkorodov, S. A. Formation of Brown Carbon Via Reactions of Ammonia with Secondary Organic Aerosols from Biogenic and Anthropogenic Precursors. *Atmos. Environ.* **2012**, *63*, 22–31.

(31) Bateman, A. P.; Walser, M. L.; Desyaterik, Y.; Laskin, J.; Laskin, A.; Nizkorodov, S. A. The Effect of Solvent on the Analysis of Secondary Organic Aerosol Using Electrospray Ionization Mass Spectrometry. *Environ. Sci. Technol.* **2008**, *42*, 7341–7346.

(32) Lignell, H.; Epstein, S. A.; Marvin, M. R.; Shemesh, D.; Gerber, B.; Nizkorodov, S. Experimental and Theoretical Study of Aqueous *cis*-Pinonic Acid Photolysis. *J. Phys. Chem. A* **2013**, *117*, 12930–12945.

(33) Madronich, S. *Tropospheric Ultraviolet and Visible (TUV) Radiation Model.* http://cprm.acd.ucar.edu/Models/TUV/index.shtml (accessed May 2014).

(34) Bateman, A. P.; Laskin, J.; Laskin, A.; Nizkorodov, S. A. Applications of High-Resolution Electrospray Ionization Mass Spectrometry to Measurements of Average Oxygen to Carbon Ratios

in Secondary Organic Aerosols. *Environ. Sci. Technol.* **2012**, *46*, 8315–8324.

(35) Bateman, A. P.; Nizkorodov, S. A.; Laskin, J.; Laskin, A. Time-Resolved Molecular Characterization of Limonene/Ozone Aerosol Using High-Resolution Electrospray Ionization Mass Spectrometry. *Phys. Chem. Chem. Phys.* **2009**, *11*, 7931–7942.

(36) Nguyen, T. B.; Bateman, A. P.; Bones, D. L.; Nizkorodov, S. A.; Laskin, J.; Laskin, A. High-Resolution Mass Spectrometry Analysis of Secondary Organic Aerosol Generated by Ozonolysis of Isoprene. *Atmos. Environ.* **2010**, *44*, 1032–1042.

(37) Nguyen, T. B.; Laskin, J.; Laskin, A.; Nizkorodov, S. A. Nitrogen-Containing Organic Compounds and Oligomers in Secondary Organic Aerosol Formed by Photooxidation of Isoprene. *Environ. Sci. Technol.* **2011**, *45*, 6908–6918.

(38) Nguyen, T. B.; Roach, P. J.; Laskin, J.; Laskin, A.; Nizkorodov, S. A. Effect of Humidity on the Composition of Isoprene Photooxidation Secondary Organic Aerosol. *Atmos. Chem. Phys.* **2011**, *11*, 6931–6944.

(39) Reemtsma, T.; These, A.; Springer, A.; Linscheid, M. Fulvic Acids as Transition State of Organic Matter: Indications from High Resolution Mass Spectrometry. *Environ. Sci. Technol.* **2006**, *40*, 5839–5845.

(40) Wozniak, A.; Bauer, J.; Sleighter, R.; Dickhut, R.; Hatcher, P. Technical Note: Molecular Characterization of Aerosol-Derived Water Soluble Organic Carbon Using Ultrahigh Resolution Electrospray Ionization Fourier Transform Ion Cyclotron Resonance Mass Spectrometry. *Atmos. Chem. Phys.* **2008**, *8*, 5099–5111.

(41) Gómez-González, Y.; Surratt, J. D.; Cuyckens, F.; Szmigielski, R.; Vermeylen, R.; Jaoui, M.; Lewandowski, M.; Offenberg, J. H.; Kleindienst, T. E.; Edney, E. O. Characterization of Organosulfates from the Photooxidation of Isoprene and Unsaturated Fatty Acids in Ambient Aerosol Using Liquid Chromatography/(−) Electrospray Ionization Mass Spectrometry. *J. Mass Spectrom.* **2008**, *43*, 371–382.

(42) Altieri, K.; Turpin, B.; Seitzinger, S. Oligomers, Organosulfates, and Nitrooxy Organosulfates in Rainwater Identified by Ultra-High Resolution Electrospray Ionization FT-ICR Mass Spectrometry. *Atmos. Chem. Phys.* **2009**, *9*, 2533–2542.

(43) Altieri, K. E.; Turpin, B. J.; Seitzinger, S. P. Composition of Dissolved Organic Nitrogen in Continental Precipitation Investigated by Ultra-High Resolution FT-ICR Mass Spectrometry. *Environ. Sci. Technol.* **2009**, *43*, 6950–6955.

(44) Smith, J. S.; Laskin, A.; Laskin, J. Molecular Characterization of Biomass Burning Aerosols Using High-Resolution Mass Spectrometry. *Anal. Chem.* **2009**, *81*, 1512–1521.

(45) Laskin, A.; Smith, J. S.; Laskin, J. Molecular Characterization of Nitrogen-Containing Organic Compounds in Biomass Burning Aerosols Using High-Resolution Mass Spectrometry. *Environ. Sci. Technol.* **2009**, *43*, 3764–3771.

(46) Mazzoleni, L. R.; Ehrmann, B. M.; Shen, X.; Marshall, A. G.; Collett, J. L., Jr. Water-Soluble Atmospheric Organic Matter in Fog: Exact Masses and Chemical Formula Identification by Ultrahigh-Resolution Fourier Transform Ion Cyclotron Resonance Mass Spectrometry. *Environ. Sci. Technol.* **2010**, *44*, 3690–3697.

(47) Mazzoleni, L. R.; Saranjampour, P.; Dalbec, M. M.; Samburova, V.; Hallar, A. G.; Zielinska, B.; Lowenthal, D. H.; Kohl, S. Identification of Water-Soluble Organic Carbon in Non-Urban Aerosols Using Ultrahigh-Resolution FT-ICR Mass Spectrometry: Organic Anions. *Environ. Chem.* **2012**, *9*, 285–297.

(48) Roach, P. J.; Laskin, J.; Laskin, A. Molecular Characterization of Organic Aerosols Using Nanospray-Desorption/Electrospray Ionization-Mass Spectrometry. *Anal. Chem.* **2010**, *82*, 7979–7986.

(49) Chang-Graham, A. L.; Profeta, L. T.; Johnson, T. J.; Yokelson, R. J.; Laskin, A.; Laskin, J. Case Study of Water-Soluble Metal Containing Organic Constituents of Biomass Burning Aerosol. *Environ. Sci. Technol.* **2011**, *45*, 1257–1263.

(50) Schmitt-Kopplin, P.; Gelencser, A.; Dabek-Zlotorzynska, E.; Kiss, G.; Hertkorn, N.; Harir, M.; Hong, Y.; Gebefugi, I. Analysis of the Unresolved Organic Fraction in Atmospheric Aerosols with Ultrahigh-Resolution Mass Spectrometry and Nuclear Magnetic Resonance

Spectroscopy: Organosulfates as Photochemical Smog Constituents. *Anal. Chem.* **2010**, *82*, 8017−8026.

(51) Rincón, A. G.; Calvo, A. I.; Dietzel, M.; Kalberer, M. Seasonal Differences of Urban Organic Aerosol Composition—An Ultra-High Resolution Mass Spectrometry Study. *Environ. Chem.* **2012**, *9*, 298−319.

(52) Lin, P.; Yu, J. Z.; Engling, G.; Kalberer, M. Organosulfates in Humic-like Substance Fraction Isolated from Aerosols at Seven Locations in East Asia: A Study by Ultra-High-Resolution Mass Spectrometry. *Environ. Sci. Technol.* **2012**, *46*, 13118−13127.

(53) O'Brien, R. E.; Laskin, A.; Laskin, J.; Liu, S.; Weber, R.; Russell, L. M.; Goldstein, A. H. Molecular Characterization of Organic Aerosol Using Nanospray Desorption/Electrospray Ionization Mass Spectrometry: Calnex 2010 Field Study. *Atmos. Environ.* **2013**, *68*, 265−272.

(54) O'Brien, R. E.; Nguyen, T. B.; Laskin, A.; Laskin, J.; Hayes, P. L.; Liu, S.; Jimenez, J. L.; Russell, L. M.; Nizkorodov, S. A.; Goldstein, A. H. Probing Molecular Associations of Field-Collected and Laboratory-Generated SOA with Nano-Desi High-Resolution Mass Spectrometry. *J. Geophys. Res. Atmos.* **2013**, *118*, 1042−1051.

(55) Kourtchev, I.; Fuller, S.; Aalto, J.; Ruuskanen, T. M.; McLeod, M. W.; Maenhaut, W.; Jones, R.; Kulmala, M.; Kalberer, M. Molecular Composition of Boreal Forest Aerosol from Hyytiälä, Finland, Using Ultrahigh Resolution Mass Spectrometry. *Environ. Sci. Technol.* **2013**, *47*, 4069−4079.

(56) Kourtchev, I.; Fuller, S.; Giorio, C.; Healy, R.; Wilson, E.; O'Connor, I.; Wenger, J.; McLeod, M.; Aalto, J.; Ruuskanen, T. Molecular Composition of Biogenic Secondary Organic Aerosols Using Ultrahigh-Resolution Mass Spectrometry: Comparing Laboratory and Field Studies. *Atmos. Chem. Phys.* **2014**, *14*, 2155−2167.

(57) Kourtchev, I.; O'Connor, I.; Giorio, C.; Fuller, S.; Kristensen, K.; Maenhaut, W.; Wenger, J.; Sodeau, J.; Glasius, M.; Kalberer, M. Effects of Anthropogenic Emissions on the Molecular Composition of Urban Organic Aerosols: An Ultrahigh Resolution Mass Spectrometry Study. *Atmos. Environ.* **2014**, *89*, 525−532.

(58) Tao, S.; Lu, X.; Levac, N.; Bateman, A.; Nguyen, T. B.; Bones, D.; Nizkorodov, S. A.; Laskin, J.; Laskin, A.; Yang, X. Molecular Characterization of Organosulfates in Organic Aerosols from Shanghai and Los Angeles Urban Areas by Nanospray-Desorption Electrospray Ionization High-Resolution Mass Spectrometry. *Environ. Sci. Technol.* **2014**, *48*, 10993−11001.

(59) Hu, K.; Darer, A. I.; Elrod, M. J. Thermodynamics and Kinetics of the Hydrolysis of Atmospherically Relevant Organonitrates and Organosulfates. *Atmos. Chem. Phys.* **2011**, *11*, 8307−8320.

(60) Darer, A. I.; Cole-Filipiak, N. C.; O'Connor, A. E.; Elrod, M. J. Formation and Stability of Atmospherically Relevant Isoprene-Derived Organosulfates and Organonitrates. *Environ. Sci. Technol.* **2011**, *45*, 1895−1902.

(61) Walser, M. L.; Park, J.; Gomez, A. L.; Russell, A. R.; Nizkorodov, S. A. Photochemical Aging of Secondary Organic Aerosol Particles Generated from the Oxidation of d-Limonene. *J. Phys. Chem. A* **2007**, *111*, 1907−1913.

(62) Glasius, M.; Lahaniati, M.; Calogirou, A.; Di Bella, D.; Jensen, N. R.; Hjorth, J.; Kotzias, D.; Larsen, B. R. Carboxylic Acids in Secondary Aerosols from Oxidation of Cyclic Monoterpenes by Ozone. *Environ. Sci. Technol.* **2000**, *34*, 1001−1010.

(63) Nguyen, T. B.; Laskin, A.; Laskin, J.; Nizkorodov, S. A. Brown Carbon Formation from Ketoaldehydes of Biogenic Monoterpenes. *Faraday Discuss.* **2013**, *165*, 473−494.

(64) Winterhalter, R.; Dingenen, R. V.; Larsen, B. R.; Jensen, N. R.; Hjorth, J. LC-MS Analysis of Aerosol Particles from the Oxidation of α-Pinene by Ozone and OH-Radicals. *Atmos. Chem. Phys. Discuss.* **2003**, *3*, 1−39.

(65) Kahnt, A.; Iinuma, Y.; Mutzel, A.; Böge, O.; Claeys, M.; Herrmann, H. Campholenic Aldehyde Ozonolysis: A Mechanism Leading to Specific Biogenic Secondary Organic Aerosol Constituents. *Atmos. Chem. Phys.* **2014**, *14*, 719−736.

(66) Hamilton, J. F.; Lewis, A. C.; Reynolds, J. C.; Carpenter, L. J.; Lubben, A. Investigating the Composition of Organic Aerosol Resulting from Cyclohexene Ozonolysis: Low Molecular Weight and Heterogeneous Reaction Products. *Atmos. Chem. Phys.* **2006**, *6*, 4973−4984.

(67) Warscheid, B.; Hoffmann, T. Direct Analysis of Highly Oxidised Organic Aerosol Constituents by On-Line Ion Trap Mass Spectrometry in the Negative-Ion Mode. *Rapid Commun. Mass Spectrom.* **2002**, *16*, 496−504.

(68) Reinhardt, A.; Emmenegger, C.; Gerrits, B.; Panse, C.; Dommen, J.; Baltensperger, U.; Zenobi, R.; Kalberer, M. Ultrahigh Mass Resolution and Accurate Mass Measurements as a Tool to Characterize Oligomers in Secondary Organic Aerosols. *Anal. Chem.* **2007**, *79*, 4074−4082.

(69) Kundu, S.; Fisseha, R.; Putman, A.; Rahn, T.; Mazzoleni, L. High Molecular Weight SOA Formation During Limonene Ozonolysis: Insights from Ultrahigh-Resolution FT-ICR Mass Spectrometry Characterization. *Atmos. Chem. Phys.* **2012**, *12*, 5523−5536.

(70) Walser, M. L.; Desyaterik, Y.; Laskin, J.; Laskin, A.; Nizkorodov, S. A. High-Resolution Mass Spectrometric Analysis of Secondary Organic Aerosol Produced by Ozonation of Limonene. *Phys. Chem. Chem. Phys.* **2008**, *10*, 1009−1022.

(71) Koch, B.; Dittmar, T. From Mass to Structure: An Aromaticity Index for High-Resolution Mass Data of Natural Organic Matter. *Rapid Commun. Mass Spectrom.* **2006**, *20*, 926−932.

(72) Zanardi-Lamardo, E.; Moore, C. A.; Zika, R. G. Seasonal Variation in Molecular Mass and Optical Properties of Chromophoric Dissolved Organic Material in Coastal Waters of Southwest Florida. *Mar. Chem.* **2004**, *89*, 37−54.

(73) Mopper, K.; Zhou, X.; Kieber, R. J.; Kieber, D. J.; Sikorski, R. J.; Jones, R. D. Photochemical Degradation of Dissolved Organic Carbon and Its Impact on the Oceanic Carbon Cycle. *Nature* **1991**, *353*, 60−62.

(74) Schmitt-Kopplin, P.; Hertkorn, N.; Schulten, H.-R.; Kettrup, A. Structural Changes in a Dissolved Soil Humic Acid During Photochemical Degradation Processes under O_2 and N_2 Atmosphere. *Environ. Sci. Technol.* **1998**, *32*, 2531−2541.

(75) Jiang, H.; Xue, H.; Teller, A.; Feingold, G.; Levin, Z. Aerosol Effects on the Lifetime of Shallow Cumulus. *Geophys. Res. Lett.* **2006**, *33*, No. L14805, DOI: 10.1029/2009GL037424.

(76) Docherty, K. S.; Wu, W.; Lim, Y. B.; Ziemann, P. J. Contributions of Organic Peroxides to Secondary Aerosol Formed from Reactions of Monoterpenes with O_3. *Environ. Sci. Technol.* **2005**, *39*, 4049−4059.

(77) Epstein, S. A.; Shemesh, D.; Tran, V. T.; Nizkorodov, S. A.; Gerber, R. B. Absorption Spectra and Photolysis of Methyl Peroxide in Liquid and Frozen Water. *J. Phys. Chem. A* **2012**, *116*, 6068−6077.

(78) Kamboures, M. A.; Nizkorodov, S. A.; Gerber, R. B. Ultrafast Photochemistry of Methyl Hydroperoxide on Ice Particles. *Proc. Natl. Acad. Sci. U. S. A.* **2010**, *107*, 6600−6604.

(79) Norrish, R. G. W.; Bamford, C. H. Photodecomposition of Aldehydes and Ketones. *Nature* **1936**, *138*, 1016.

(80) von Sonntag, C.; Schuchmann, H.-P. The Elucidation of Peroxyl Radical Reactions in Aqueous Solution with the Help of Radiation-Chemical Methods. *Angew. Chem., Int. Ed. Engl.* **1991**, *30*, 1229−1253.

(81) Ingold, K. U. Peroxy Radicals. *Acc. Chem. Res.* **1969**, *2*, 1−9.

(82) Ashmore, P. G.; Sugden, T.; Dainton, F. *Photochemistry and Reaction Kinetics*; Cambridge University Press: Cambridge, U.K., 1967.

(83) Nguyen, T. B.; Nizkorodov, S. A.; Laskin, A.; Laskin, J. An Approach toward Quantification of Organic Compounds in Complex Environmental Samples Using High-Resolution Electrospray Ionization Mass Spectrometry. *Anal. Methods* **2013**, *5*, 72−80.

(84) Aiken, A. C.; DeCarlo, P. F.; Jimenez, J. L. Elemental Analysis of Organic Species with Electron Ionization High-Resolution Mass Spectrometry. *Anal. Chem.* **2007**, *79*, 8350−8358.

(85) Aiken, A. C.; DeCarlo, P. F.; Kroll, J. H.; Worsnop, D. R.; Huffman, J. A.; Docherty, K. S.; Ulbrich, I. M.; Mohr, C.; Kimmel, J. R.; Sueper, D. O/C and OM/OC Ratios of Primary, Secondary, and Ambient Organic Aerosols with High-Resolution Time-of-Flight Aerosol Mass Spectrometry. *Environ. Sci. Technol.* **2008**, *42*, 4478−4485.

(86) DeCarlo, P. F.; Kimmel, J. R.; Trimborn, A.; Northway, M. J.; Jayne, J. T.; Aiken, A. C.; Gonin, M.; Fuhrer, K.; Horvath, T.; Docherty, K. S. Field-Deployable, High-Resolution, Time-of-Flight Aerosol Mass Spectrometer. *Anal. Chem.* **2006**, *78*, 8281−8289.

(87) Alif, A.; Pilichowski, J.-F.; Boule, P. Photochemistry and Environment XIII: Phototransformation of 2-Nitrophenol in Aqueous Solution. *J. Photochem. Photobiol., A* **1991**, *59*, 209−219.

(88) Lipczynska-Kochany, E. Degradation of Nitrobenzene and Nitrophenols by Means of Advanced Oxidation Processes in a Homogeneous Phase: Photolysis in the Presence of Hydrogen Peroxide Versus the Fenton Reaction. *Chemosphere* **1992**, *24*, 1369−1380.

(89) Albinet, A.; Minero, C.; Vione, D. Phototransformation Processes of 2,4-Dinitrophenol, Relevant to Atmospheric Water Droplets. *Chemosphere* **2010**, *80*, 753−758.

2606

dx.doi.org/10.1021/jp509476r | *J. Phys. Chem. A* 2015, 119, 2594−2606